Molecular Biology Reports
https://doi.org/10.1007/s11033-022-07956-3

ORIGINAL ARTICLE

Functional EGF domain of the human neuregulin 1α produced in *Escherichia coli* with accurate disulfide bonds

Arthur Schveitzer Ferreira[1,2] · Amanda Lopacinski[1,2] · Michel Batista[3] · Priscila Mazzocchi Hiraiwa[1] · Natalia Fernanda Bueno[4] · Beatriz Gomes Guimarães[1] · Nilson I. T. Zanchin[1,2]

Received: 14 March 2022 / Accepted: 17 September 2022

Abstract

Background Neuregulins comprise a large family of growth factors containing an epidermal growth factor (EGF) domain. NRG1 acts in signaling pathways involved in proliferation, apoptosis, migration, differentiation, and adhesion of many normal cell types and in human diseases. The EGF domain of NRG1 mediates signaling by interaction with members of the ErbB family of receptors. Easy access to correctly folded hNRG1α EGF domain can be a valuable tool to investigate its function in different cell types.

Materials and methods The EGF domain of hNRG1α was produced in *Escherichia coli* in fusion with TrxA and purified after cleavage of TrxA. Conformation and stability analyses were performed by using biophysical methods and the disulfide bonds were mapped by mass spectrometry. The activity of the hNRG1α EGF domain was demonstrated in cell proliferation and migration assays.

Results Approximately 3.3 mg of hNRG1α EGF domain were obtained starting from a 0.5 L of *E. coli* culture. Correct formation of the three disulfide bonds was demonstrated by mass spectrometry with high accuracy. Heat denaturation assays monitored by circular dichroism and dynamic light scattering revealed that it is a highly stable protein. The recombinant EGF domain of hNRG1α purified in this work is highly active, inducing cell proliferation at concentration as low as 0.05 ng/mL. It induces also cell migration as demonstrated by a gap closure assay.

Conclusion The EGF domain of hNRG1α was produced in *E. coli* with the correct disulfide bonds and presented high stimulation of HeLa cell proliferation and NDFH cell migration.

Keywords Human Neuregulin-1 · Recombinant EGF domain · Disulfide bond assignment · hNRG1α EGF domain activity

Introduction

Neuregulins (NRG) comprise a large family of growth factors encoded by six genes (NRG1-NRG6) with the number of isoforms being amplified by a large number of alternative splicing events. The isoforms differ in amino acid sequence, overall structure, and levels of expression in different tissues [1]. They share an epidermal growth factor (EGF) domain that mediates cell signaling by interaction with members of the ErbB family of cellular receptors [2–4]. The EGF domain of NRG1 stimulates ErbB tyrosine kinase receptors of signaling pathways involved in cell proliferation, apoptosis, migration, differentiation, and adhesion [2–5]. NRG1 has been implicated in development of breast, heart, muscle, and brain tissues and in human diseases including breast cancer [5]. Furthermore, NRG1–ErbB4 signaling is involved in important processes

Arthur Schveitzer Ferreira and Amanda Lopacinski contributed equally to this work.

✉ Nilson I. T. Zanchin
nilson.zanchin@fiocruz.br

[1] Laboratory of Structural Biology and Protein Engineering, Carlos Chagas Institute, FIOCRUZ Paraná, Curitiba, PR, Brazil

[2] Cellular and Molecular Biology Graduate Program, Federal University of Paraná, Curitiba, PR, Brazil

[3] Mass Spectrometry Facility, Carlos Chagas Institute, FIOCRUZ Paraná, Curitiba, PR, Brazil

[4] Integrated Structural Biology Platform, Carlos Chagas Institute, FIOCRUZ Paraná, Curitiba, PR, Brazil

Published online: 05 October 2022

required for brain development and plasticity and neuropsychiatric disorders [2–4].

Six different types of NRG1 (Types I-VI) have been identified, containing distinct N-terminal regions. They are synthesized as transmembrane precursor proteins, which subsequently undergo proteolytic processing on the C-terminal region of the EGF, releasing the EGF signaling domain with the type-specific N-terminal region, except for type III, that remains bound to the membrane due to a transmembrane domain in its N-terminal region [2, 3, 6]. The EGF domain of neuregulins was shown to be sufficient to activate ErbB receptors in a specific manner and induce cellular responses [7, 8]. This favors the functional studies which require the utilization of recombinant neuregulin EGF domains, since some features of this domain, such as small size and absence of glycosylation sites, facilitates its recombinant production in prokaryotes such as *Escherichia coli* [9, 10]. In this scenario, the advantages of using *E. coli* as the host system are well known and include fast growth, cheapest growth media components, simplest laboratory setup, easy and fast transformation with exogenous DNA [11]. Nonetheless, this expression system has its specific disadvantages, particularly, the formation of inclusion bodies, which in turn, makes the process of protein purification more complex and time-consuming by requiring in vitro refolding of the recombinant proteins, which is not always possible. Several studies have reported overexpression of the EGF domain for various members of the EGF family of growth factors [12–14], however, only relatively low yields were obtained.

Despite small size, the EGF domain displays a complex structure maintained by three disulfide bonds formed by the $C_1 \times 7C_2 \times 4\text{-}5C_3 \times 10\text{-}13C_4XC_5 \times 8C_6$ conserved sequence, and with its correct folding being dependent on the accurate formation of disulfide bonds linking the cysteine residues in the combinations C1-C3, C2-C4 and C5-C6 [15]. In fact, accurate formation of the disulfide bonds may be one of the major limitations to produce soluble and functional EGF domains in procaryotes such as *E. coli*. However, it is possible to overcome this limitation by using fusion proteins, which can function as folding and solubility chaperones or modified *E. coli* strains designed to favor disulfide bond formation. Indeed, several studies described the fusion of EGF domains with different expression tags, such as SUMO for hHB-EGF [16], oleosin for hEGF [17], glutathione S-transferase, B1 domain of streptococcal protein G and protein disulfide isomerase for hEGF [18] and, thioredoxin (Trx) for hEPR [19] and for seven members of the EGF family of growth factors [20]. In addition to the use of fusion proteins to improve solubility, it is also important to demonstrate that the recombinant proteins intended for biological applications display correct structural conformation and do not form aggregates. For this, a number of methods can be applied, including size exclusion chromatography, dynamic light scattering, circular dichroism and mass spectrometry [21].

In this work, we describe the expression of the human NRG1α EGF domain fused to TrxA in *E. coli* and a two-step procedure to separate the fusion protein and purify the hNRG1α EGF domain. Yields in the range of ~6.5 mg per liter of culture were obtained after purification. More importantly, we demonstrate by mass spectrometry that the disulfide bonds are formed between the correct cysteine pairs, assuring that our strategy leads to the production of accurately folded EGF NRG1α domain. In addition, we show that the recombinant hNRG1α EGF domain presents biological activity in cell proliferation and migration assays. Our study describes a useful method to obtain biologically active EGF domains.

Materials and methods

Protein expression and purification

We used the NMR structure of the hNRG1α EGF domain deposited at the Protein Data Bank with the code 1HRE [22] to define the amino acid sequence to be expressed. A synthetic gene encoding this 67-residue segment was acquired from GenScript (Piscataway, NJ, USA) cloned between the *Nco*I and *Xho*I restriction sites of plasmid pET32a (Novagen/Merck, Darmstadt, Germany). The expression plasmids for EGF and TGFα in fusion with TrxA (pET32a-EGF and pET32a-TGFα) were described in a previous study from our group [20]. In pET32a, the EGF domain of these growth factors are expressed in fusion with thioredoxin and a hexahistidine tag. Thrombin and enterokinase cleavage sites allow separation of the hNRG1α EGF domain from TrxA-His6. For expression of hNRG1α without TrxA, the coding sequence of the hNRG1α EGF domain was excised from plasmid pET32a-hNRG1α by digestion with the restriction enzymes *Nco*I and *Hind*III and inserted into the same sites of plasmid pET28a. The resulting plasmid, pET28a-hNRG1α expresses the EGF domain of hNRG1α with a hexahistidine tag at the C-terminal. The EGF domain of EGF and TGFα were cloned into the plasmids pET22b and pET28a, respectively. In both cases, synthetic coding sequences were inserted into the *Nco*I and *Not*I restriction sites of pET22b and pET28a, respectively. In pET22b, the EGF domain of EGF is expressed with an N-terminal *pel*B signal peptide and a hexahistidine tag at the C-terminal. In pET28a, the EGF domain of TGFα is expressed with a C-terminal hexahistidine tag. The nucleotide and amino acid sequences of all EGF domains used in this work are described in the Supplementary Information file.

For evaluation of the solubility of the different EGF domain constructs, the six plasmids were transformed into

the *E. coli* strain BL21(DE3)-*ΔslyD* using a heat shock protocol as previously described [23]. The transformed cells were plated on Lysogeny Broth (LB)-agar plates containing 100 µg/mL of ampicillin (for pET22b and pET32a) or 50 µg/mL of kanamycin (for pET28a) and incubated overnight at 37 °C. A single colony was used to inoculate 10 mL of LB containing the appropriate antibiotic as described above. After incubation of this starting culture overnight at 37 °C, 1 mL were used to inoculate a 100 mL LB culture containing the appropriate antibiotic. This culture was maintained at 37 °C until the optical density at 600_{nm} reached ~ 0.6. Subsequently, the culture was transferred to 16 °C, induced with 0.3 mM IPTG and incubated further at 16 °C for 24 h with rapid agitation (300 rpm). Subsequently, the bacterial cells were harvested by centrifugation at 6,000 x g for 10 min at 4 °C, suspended in 1 mL of lysis buffer (20 mM Tris.HCl pH 8.0; 200 mM NaCl; 20 mM imidazole) and lysed by four freezing-thawing cycles. The lysates were homogenized using a Q700 sonicator (QSonica, Newtown, CT, USA) and a 3 mm tip with amplitude 10, during six cycles of 30 s with 1-minute intervals. The lysates were cleared by centrifugation at 20,000 x g for 10 min at 4 °C and the extracts transferred to a new Eppendorf tube. The pellets were washed twice with 1 mL of lysis buffer containing 2% Triton X-100 (v/v) with three cycles of sonication and the insoluble fraction was sedimented by centrifugation at 20,000 x g for 10 min at 4 °C. For comparison, the insoluble fraction was suspended in 1 mL of lysis buffer. 5 µL of both soluble and insoluble fractions were analyzed by SDS-PAGE in gel containing either 13% (w/v) of polyacrylamide for the EGF growth factors domains fused to TrxA or 15% (w/v) of polyacrylamide for the EGF domains without TrxA fusion.

For purification of hNRG1α, the plasmid pET32a-hNRG1α was transformed into the *E. coli* expression strain SHuffle (NEB C3026J) [24]. The transformed cells were plated on Lysogeny Broth (LB)-agar plates containing 100 µg/mL of ampicillin and incubated overnight at 37 °C. A single colony was used to inoculate 10 mL of LB containing 100 µg/mL of ampicillin. After incubation of this starting culture overnight at 37 °C, 5 mL were used to inoculate a 500 mL LB culture containing 100 µg/mL of ampicillin. This culture was maintained at 37 °C until the optical density at 600_{nm} reached ~ 0.6. Subsequently, the culture was transferred to 16 °C, induced with 0.5 mM IPTG and incubated further at 16 °C for 24 h with rapid agitation (300 rpm).

Following induction, the bacterial cells were harvested by centrifugation at 6,000 x g for 10 min at 4 °C. The cells were suspended in 10 mL of buffer A (50 mM Tris.HCl pH 8.0; 300 mM NaCl; 20 mM imidazole), lysed using a microfluidizer (Microfluidics, Newton, MA, USA) and the extract was cleared by centrifugation at 20,000 x g for 30 min. The Trx-hNRG1α EGF domain fusion protein was purified by affinity chromatography using a HisTrap 5 mL column (Cytiva 17,524,802) on an ÄKTA Pure M25 chromatography system (Cytiva, Marlborough, USA). After loading the sample, the column was washed using 3 column volumes (CV) of buffer A, followed by a 0 to 10% gradient of buffer B (50 mM TrisHCl pH 8.0; 300 mM NaCl; 500 mM imidazole) in two CV. The target protein was eluted using a 10 to 100% gradient of buffer B in four CV. The peak fractions were combined after analysis by SDS-PAGE. Five mL of the sample were diluted to a final volume of 15 mL using 50 mM Tris-HCl pH 8.0 and 300 mM NaCl. Protein concentration was determined based on absorbance at 205 nm and the extinction coefficient using a NanoDrop ONE^c Spectrophotometer (Thermo Fisher Scientific, Waltham, MA, USA). The thioredoxin-tag was removed by digestion with one unit of thrombin (Cytiva 27,084,601) for each 10 mg of recombinant TrxA-hNRG1α EGF domain fusion protein at 25 °C for 20 h. After thrombin digestion, TrxA containing the hexa-histidine tag was removed by affinity chromatography using the same protocol described above. The flowthrough sample, containing the hNRG1α EGF domain devoid of the fusion sequences, was concentrated using an Amicon Ultra-0.5 mL 3 K (Merk Millipore, Cork Ireland) to a final volume of 500 µL and purified further by size-exclusion chromatography using a Superdex 75 10/300 GL column (Cytiva 29,148,721). After each chromatographic step, the samples were analyzed by SDS-PAGE. Poly-acrylamide concentrations in the stacking and separating gels were 6.5% and 15%, respectively. Electrophoresis was performed with 0.75 mm-thick gels assembled on Mini-PROTEAN Tetra Cells (Bio-Rad Laboratories, Hercules, USA) at 100 V. Gels were stained using Brilliant Blue R-250 and destained using a methanol/acetic acid/water (30%/10%/60%, v/v) solution.

Limited proteolysis assay

Limited proteolysis assays were performed under reducing and non-reducing conditions. For reduction of the disulfide bonds, the recombinant hNRG1α EGF domain was treated with 10 mM of dithiothreitol (DTT, Merck 3483123). The limited proteolysis assays were performed with a 100:1 (w/w) ratio of recombinant hNRG1α EGF domain and trypsin (Sigma 59427 C) and incubated for 30 and 60 min at 37 °C. Control reactions without trypsin were run in parallel. The products of the reactions were analyzed by SDS-PAGE.

Determination of Disulfide Bonds by Mass Spectrometry

For sample preparation, 5 µg of unreduced recombinant hNRG1α EGF domain were incubated in 6 M urea, 5 mM NEM for 15 min at RT, digested for 4 h at 37 °C with 0.1 µg Lys-C, diluted 1:8 with PBS, incubated with 0.17 µg of Glu-C at 37 °C overnight and inactivated with 0.5% TFA.

Proteolysis products were desalted using C18 stage tips and the eluates from the stage tips concentrated by speed vac. Hundred nanograms of digested peptides were submitted to LC-MS/MS using an Ultimate 3000 RSLCnano system coupled to an Orbitrap Fusion Lumos (Thermo Fischer Scientific, Waltham, MA, USA). For ESI LC HCD, the liquid chromatography analysis was performed on an ACQUITY UPLC CSH C18 column, (100 mm length, 2.1 mm I.D., particles with 1.7 micrometers; Waters, Milford, MA, USA) with a flow of 100 µL/min and a gradient from 5 to 40% MeCN, in 0.1% formic acid for 90 min. Data acquisition was done in DDA mode with MS1 and MS2 (post HCD fragmentation) spectra acquired in the orbitrap set to 120k resolution with automatic gain control of 4×10^5 and maximum injection time of 200 ms or 240 ms, respectively. In nano LC EThcD analysis, peptide separation was performed using a homemade C18 packed emitter (150 mm length, 75 um I.D., particles with 3 micrometers) (Dr. Maisch, Ammerbuch-Entringen, Germany) with a flow of 250 nL/min, a gradient from 5 to 40% MeCN, 0.1% formic acid for 30 min. The acquisition was done in DDA mode with MS1 spectra acquired in the orbitrap set to 120k resolution with automatic gain control standard and maximum injection time of 50 ms. Fragmentation was done using EThcD, MS2 in the orbitrap set to 30k resolution with automatic gain control standard, and maximum injection time of 54 ms. Raw data were analyzed in BioPharma Finder 3.0 and the disulfide bond sites identified fit the follow criteria: up to 3 disulfide bonds per peptide; MS2 identification performed, and precursor mass error ≤ 5 ppm.

Dynamic light scattering and thermal unfolding analyses

Dynamic Light Scattering (DLS) and thermal unfolding were performed on a Prometheus Panta device (Nanotemper Technologies, Munich, Germany) using standard capillaries. DLS measurements were performed at 20 °C using the high sensitivity setup (10 acquisitions of 10 s each) in duplicates. Non-reduced samples of the hRG1α EGF domain were also submitted to a linear ramp of 1 °C/min from 20 to 95 °C, and back to 20 °C, with parallel measurement of DLS.

Circular dichroism

For circular dichroism analyses, the sample buffer was changed by ultrafiltration to 4.2 mM Tris-HCl pH 8.0 and 50 mM NaCl using Amicon Ultra-0.5 mL 3 K concentrators (Merk Millipore, Cork Ireland). CD spectra were acquired using the hRG1α EGF domain at 0.2 mg/mL using a 1 mm path cuvette on a Jasco J-815 circular dichroism spectrometer (JASCO, Tokyo, Japan) with a scanning speed of 50 nm/min at 20 °C. Each spectrum was accumulated at least five times in the range from 190 to 260 nm. For thermal denaturation, the temperature was raised from 20 to 80 °C. A new set of spectra was acquired after cooling to 20 °C. The raw data were converted using the mean residue molar ellipticity formula and autozero was set by using the value at 250 nm.

Cell proliferation assay

HeLa cells (Carlos Chagas Institute cell bank) were cultivated in DMEM (Thermo Fisher Scientific 41,965,062) supplemented with 10% fetal bovine serum (FBS) at 37 °C with 80% humidity and 5% CO_2 using a Forma Series II Water Jacketed CO_2 incubator (Thermo Fischer Scientific, Waltham, MA, USA). Subsequently, cells from a confluent culture were transferred to a 24-well plate at a concentration of 10^5 cells per well and incubated for 24 h. The medium was changed for DMEM without FBS and treated with 50 ng/mL of recombinant hNRG1α EGF domain in triplicates in parallel with untreated controls also in triplicates. After 48 h, the wells were washed with PBS (137 mM NaCl, 2.7 mM KCl, 8 mM Na_2HPO_4, and 2 mM KH_2PO_4) and treated with 200 µL of PBS containing trypsin 1% (w/v) (Merck T8003). After 5 min of incubation at 37 °C, the released cells were collected, centrifuged at 500 x g for 5 min and suspended in 280 µL of PBS and 20 µL of *CountBright*™ *Absolute Counting Beads* (Thermo Fisher C36950). The cell number was determined on a BD FACS Canto II (BD Life Sciences, New Jersey, USA) and the results analyzed using the software FlowJo™ v10.8 (BD Life Sciences, Franklin Lakes, NJ, USA). At least 1000 beads were acquired and a maximum of 3000 beads was set as upper limit. Quantification was performed following the protocol described at the *CountBright*™ *Absolute Counting Beads* manual (Invitrogen MAN0018850). The one-way ANOVA with Dunnett post-test was performed by comparing the means between the groups.

A dose response curve of the effect of the recombinant hNRG1α EGF domain on HeLa cell proliferation was determined by the 3-[4,5-dimethylthiazol-2-yl]-2,5 diphenyl tetrazolium bromide (MTT) viability cell assay. For this purpose, HeLa cells were cultivated in 96-well plates in as described above for the proliferation assay. The assay was performed in triplicate utilizing 5×10^4 cells per well and increasing concentrations of the recombinant hNRG1α EGF domain: 0.005 ng/mL, 0.05 ng/mL, 0.5 ng/mL, 5 ng/mL and 50 ng/mL. After 48 h of incubation, the wells were washed with PBS, treated with 50 µL of MTT (Invitrogen M6494) at 5 mg/mL and 50 µL of serum free medium and incubated at 37 °C for 3 h. Subsequently, 150 µL of a solvent solution (4 mM HCl, 0.1% NP40 in isopropanol) was added to each well and incubated for another hour. Absorbance was read at 570 nm using a Synergy H1 Hybrid Reader (BioTek Instruments,

Winooski, VT, USA). The dose-response curve was adjusted using a nonlinear fit of the data.

Scratch closure assay

NDFH cells (Lonza CC-2509) were maintained in DMEM (Thermo Fisher 41,965,062) supplemented with 10% FBS at 37 °C with 80% humidity and 5% CO_2 using a Forma Series II Water Jacketed CO_2 incubator (Thermo Fischer Scientific, Waltham, MA, USA). For scratch closure assays, the cells were allowed to grow to ~ 100% confluence when the medium was changed to DMEM without FBS and, the incubation continued for further 24 h. At this time, a scratch was made at the center of the well, 50 ng of recombinant hNRG1α EGF domain were added to cultures and images of the unstained cells were acquired. Each treatment was performed in triplicate. After 48 h, the cells were stained using the crystal violet protocol described by Feoktistova et al. [25]. Briefly, the cells were initially fixed using ice-cold 100% methanol for 10 min, stained with a 0.5% (w/v) crystal violet solution in 20% (v/v) methanol for 10 min and washed with PBS. Images of the stained cells were acquired on a Nikon Eclipse TE300 Inverted Microscope (Nikon, Tokyo, Japan) using a 10X objective and the QCapture Pro 6.0 software (Teledyne QImaging, Surrey, Canada). The rate of wound healing was calculated using ImageJ [26]. The scratches were aligned with the base of the image and a 900 × 600-pixel rectangle was cropped around the scratch. The area at time 0 was calculated using the polygon selection tool and the area at 48 h was calculated using the area between the edges of the scratch converted to an 8-bit image, which is sharpened afterwards. The find edges tool was applied and the image was converted to binary format. The particles were then analyzed using areas between 30 and 100,000 $inch^2$ with bare outlines, including holes and the values obtained using the summarize tool.

Results

High yields of hNRG1α EGF domain obtained from *E. coli* expression.

The EGF domain of hNRG1α (amino acid sequence according to Protein Data Bank code 1HRE) [22] was expressed in fusion with thioredoxin A (TrxA), which contributes to correct protein folding and solubility [27], using the pET32a plasmid and the *E. coli* expression strain SHuffle (NEB C3026J) [24]. The positive effect of TrxA fusion on the solubility of the EGF domain of the growth factors hNRG1α, EGF and TGFα expressed in *E. coli* can be seen in Fig. 1 A and 1B. All EGF domains in fusion with TrxA are highly soluble but when expressed without the TrxA fusion they are found mostly in the insoluble faction. The segment between TrxA and the hNRG1α EGF domain contains a hexa-histidine tag to facilitate purification by affinity chromatography on immobilized metal columns and, thrombin and enterokinase cleavage sites allowing for subsequent cleavage and separation of the fusion protein. High levels of purified fusion protein were obtained after affinity chromatography, which migrates as a single band of approximately 30 kDa in SDS-PAGE (Fig. 1 C). TrxA was efficiently cleaved by thrombin digestion. However, TrxA-Hisx6 and the hNRG1α EGF domain co-migrate with apparent molecular masses of ~ 15 kDa in 15% SDS-PAGE (Fig. 1D, lane 1). Nevertheless, TrxA-Hisx6 was efficiently separated from the hNRGα EGF domain by a second round of purification on an immobilized nickel column (Fig. 1D), which retained TrxA-Hisx6. The hNRG1α EGF domain found in the flow through of the second affinity chromatography was further purified by size-exclusion chromatography (Fig. 1D and E). A major peak eluted with the expected volume for the monomeric conformation of the hNRG1α EGF domain (Fig. 1E). TrxA has a distinct elution profile in the Superdex 75 10/300 column, which is clearly distinguishable from the hNRG1α EGF domain elution profile (data not shown). Although it is a two-step purification protocol, this process is significantly less cumbersome than in vitro refolding of denatured proteins, especially considering the need for accurate disulfide bond formation. We obtained ~ 3.3 mg of recombinant hNRG1α EGF domain starting from 10 mg of protein before thrombin digestion and from 500 mL of *E. coli* cell culture.

Stability and conformational analysis of the recombinant hNRG1α EGF domain

Conformation of the recombinant hNRG1α EGF domain was initially assessed by limited proteolysis assays. This type of assay can provide indirect information on protein conformation since unstructured or unfolded regions are more accessible to the protease, being digested at faster rates than compact, well-structured regions. Considering that the EGF domain comprises the conserved sequence $C_1 \times 7C_2 \times 4\text{-}5C_3 \times 10\text{-}13C_4XC_5 \times 8C_6$ [15] and its correct folding is dependent on the correct formation of disulfide bonds linking the cysteine residues in the combinations C1-C3, C2-C4, C5-C6, limited proteolysis assays were performed with recombinant factors previously treated with DTT in parallel with control samples, which were not treated with reducing agent (Fig. 2 A). Treatment of the hNRG1α EGF domain with reducing agents, such as DTT, is expected to disrupt the disulfide bonds, which may lead to complete unfolding of the domain. Consistently, the reduced hNRG1α EGF domain showed high sensitivity to trypsin, being totally degraded after 30 min of incubation, while the non-reduced

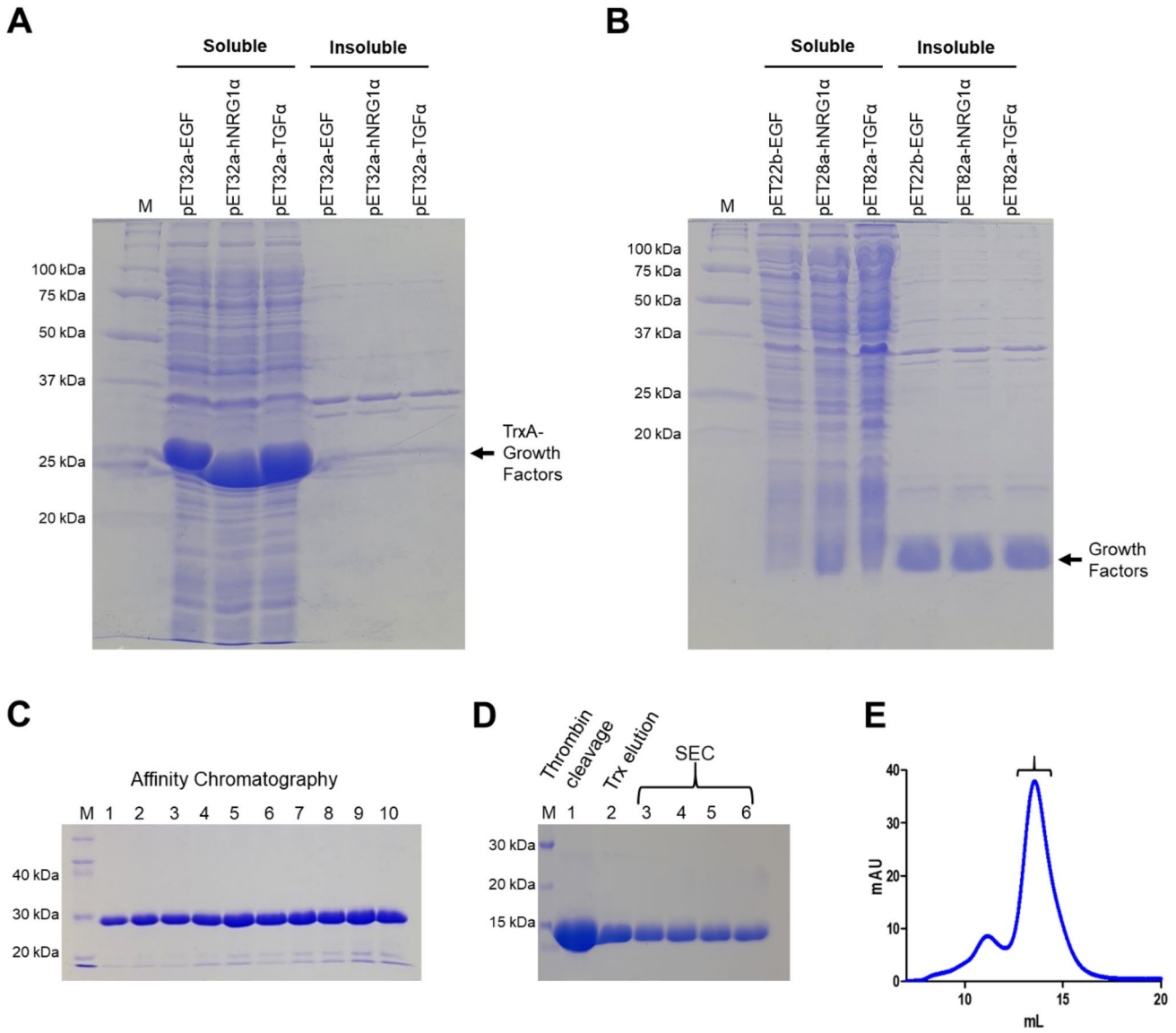

Fig. 1 Expression of the EGF domains of EGF, hNRG1α and TGFα and purification of the hNRG1α EGF domain. **A** Expression of the EGF domains of the growth factors EGF, hNRG1α and TGFα in fusion with TrxA using plasmid pET32a. Most of the recombinant EGF growth factor domains are found in the soluble extract. **B** Expression of the EGF domain of the growth factor EGF with the N-terminal *pel*B signal peptide and a C-terminal hexahistidine tag using plasmid pET22b and, of the EGF domains of hNRG1α and TGFα a C-terminal hexahistidine tag using plasmid pET28a. Most of the recombinant EGF growth factor domains are found in the insoluble fraction. **C** SDS-PAGE analysis of the fusion protein TrxA-hNRG1α EGF domain purified by affinity chromatography on an immobilized nickel column. **D** SDS-PAGE analysis of the thrombin digestion product (lane 1), TrxA-Hisx6 eluted after a second round of nickel affinity chromatography (lane 2), and hNRG1α EGF domain fractions eluted from size exclusion chromatography (lanes 3–6). M, molecular mass. **E** Elution profile of the hNRG1α EGF domain fractionated on a Superdex 75 10/300 GL size-exclusion column. The samples loaded in the lanes 3–6 shown in (**D**) correspond to the major peak of the chromatogram indicated by the bracket

control was resistant to trypsin for up to 60 min of incubation (Fig. 2 A). This result provided the first indication that the cysteines are forming disulfide bonds and that hNRG1α EGF domain presents a compact conformation.

The effect of the reducing agent on the conformation of the hNRG1α EGF domain was also evaluated by dynamic light scattering (DLS). Surprisingly, in all conditions tested, including incubation with a reducing agent for 44 h, the hNRG1α EGF domain showed a single peak with radius size centered at ~2.6 nm, except for one minor peak after 44 h indicating partial aggregation (Fig. 2 C). These results show that the hNRG1α EGF domain is not prone to aggregation even after disruption of the disulfide bonds. Increasing the temperature from 20 to 95 °C also did not result in an

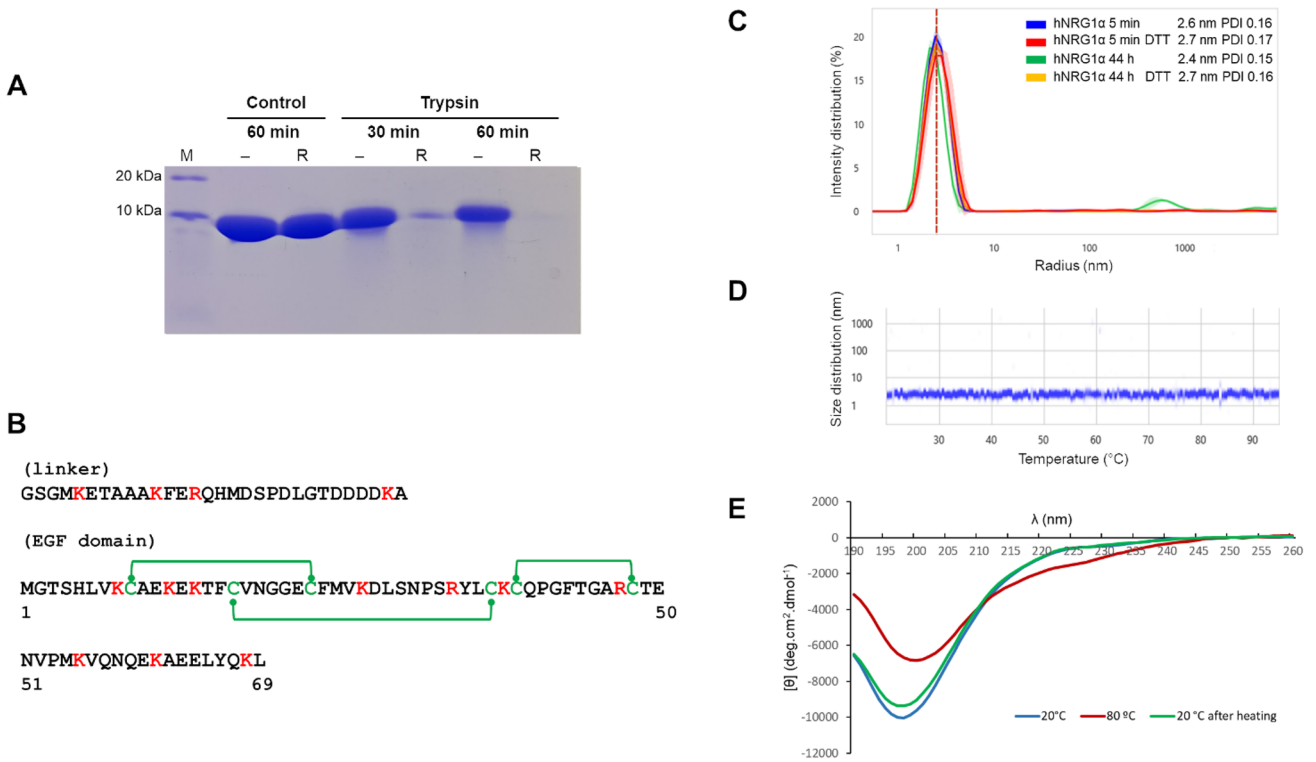

Fig. 2 Stability and conformational analysis of the hNRG1α EGF domain. **A** Limited proteolysis assays performed with samples untreated (-) and treated (+) with the reducing agent DTT and incubated for 30 and 60 min with trypsin. Control refers to the indicated conditions in the absence of trypsin. M, molecular mass markers. Only the relevant part of the gel is shown. **B** Sequence of the hNRG1α EGF domain with the basic residues targeted by trypsin marked in red and the cysteine residues marked in green. Green lines indicate the disulfide bonds. The sequence identified by (linker) represents the part of the linker encoded by the vector which remains attached to the growth factors after thrombin digestion. **C** Profiles of radius of the hNRG1α EGF domain in presence or absence of DTT as determined by dynamic light scattering analyses. The graphic shows the intensity distribution (%) as a function of particle radius (nm). All assays were performed at 20 ºC. Times and treatment are indicated in the figure as well as the corresponding cumulant radius and polydispersity index (PDI). **D** Size distribution (nm) of the hNRG1α EGF domain as determined by DLS as a function of the temperature. **E** Circular dichroism analysis of the hNRG1α EGF domain. The blue line corresponds to the spectrum acquired at 20 °C, the red line to the spectrum acquired 80 °C and the green line corresponds to the spectrum acquired at 20 °C after sample heating up to 80 °C. The far-UV circular dichroism spectra (195–260 nm) were recorded using a J-815 spectropolarimeter with five accumulations and using a 1 mm path length cell

increase in the size distribution of hNRG1α EGF domain (Fig. 2D).

To obtain additional information about the conformational stability, we measured circular dichroism (CD) spectra of the hNRG1α EGF domain in the far-UV region at 20 °C, after sample heating to 80 °C and, after returning the temperature down to 20 °C (Fig. 2E). Thermal denaturation is indicated by a reduction of the CD signal in the 200 nm wavelength range at 80 °C. However, the CD spectrum acquired after returning the temperature to 20 °C overlaps with the spectrum previously obtained at 20 °C (Fig. 2E), indicating that the hNRG1α EGF domain acquires the same conformation after thermal denaturation. That result is similar to the CD spectra found for hAREG hBTC, HB-EGF and hTGFα [20] in similar conditions.

Recombinant hNRG1α EGF domain presents accurate disulfide bonds

To confirm the correct pairing of cysteines forming disulfide bonds, the purified hNRG1α EGF domain was submitted to mass spectrometry analysis. The conserved C1-C3, C2-C4, C5-C6 cysteine pairs are numbered according to the sequence shown in Fig. 2B, corresponding to C39-C53, C47-C67 and C69-C78. The proteases Lys-C and Glu-C were selected for digestion based on the amino acid sequence of the hNRG1α EGF domain. The hinge residue between C67 and C69, as well as the sequence between C47 and C53 are the major points of constraint regarding site-specific proteolytic digestion of the hNRG1α EGF domain since, under non-reducing conditions, ineffective digestion leads to complex mass and peptides with more than two cysteines in the top score peptides. Nevertheless,

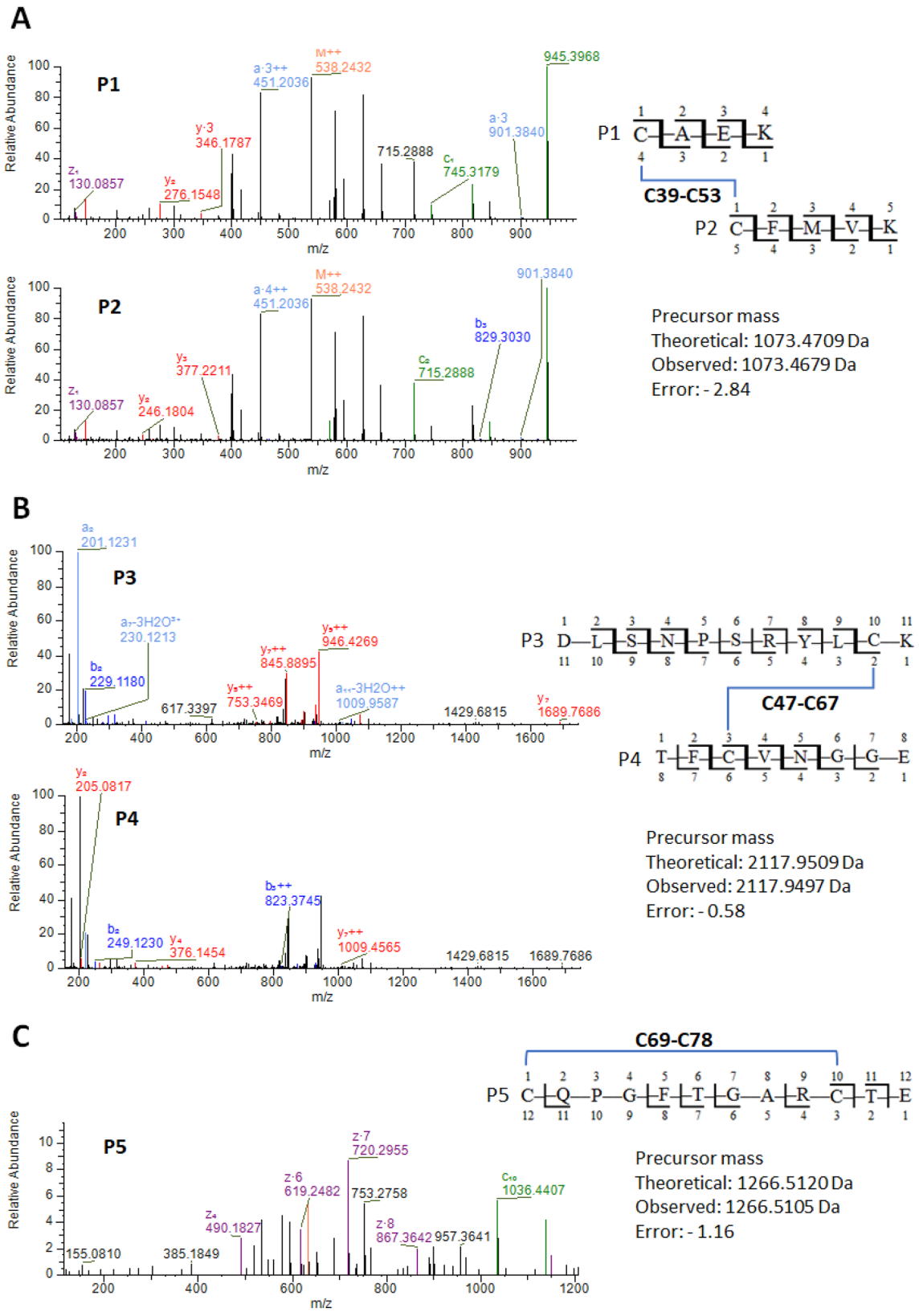

Fig. 3 Assignment of the MS/MS spectra of the disulfide bond-containing peptides of the recombinant hNRG1α EGF domain. The three disulfide bonds C39-C53 **A**, C47-67 **B** and C68-C78 **C** were identified by MS/MS. Peptides P1 and P2 were identified in the same spectra (**A**), however they were annotated separately. The same is valid for P3 and P4 (**B**). MS2 obtained with nano LC EThcD (**A** and **C**) or ESI LC HCD (**B**). Precursor mass errors reported in ppm

Table 1 List of fragment ions annotated in the MS/MS spectra of the peptides identified with one disulfide bond each as shown in Fig. 3

Disulfide bond	Fragmention*	Fragment sequence	m/z
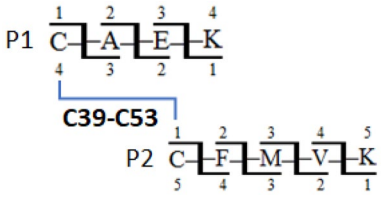	a·3++ (P1)	CAE/CFMVK	451.2036
	a·3+ (P1)	CAE/CFMVK	901.3849
	c1+ (P1)	C/CFMVK	745.3179
	y2+ (P1)	EK	276.1548
	y·3+ (P1)	AEK	346.1787
	z1+ (P1)	K	130.0857
	a·4++ (P2)	CAEK/CFMV	451.2036
	b3+ (P2)	CAEK/CFM	829.3030
	y2+ (P2)	VK	246.1804
	y3+ (P2)	MVK	377.2221
	z1+ (P2)	K	130.0857
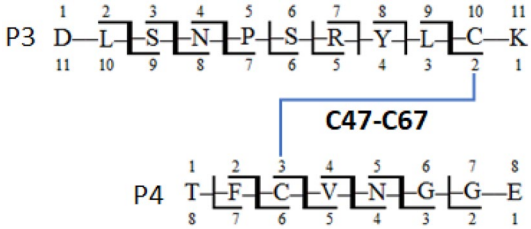	a2+ (P3)	DL	201.1231
	a7 -3H2O+++ (p3)	DLSNPSR	230.1213
	a11 -3H2O++ (p3)	DLSNPSRYLCK/TFCVNGGE	1009.9587
	b2+ (P3)	DL	229.1180
	y5++ (P3)	RYLCK/TFCVNGGE	753.3469
	y7++ (P3)	PSRYLCK/TFCVNGGE	845.8895
	y7+ (P3)	PSRYLCK/TFCVNGGE	1689.7686
	y9++ (P3)	SNPSRYLCK/TFCVNGGE	946.4269
	b2+ (P4)	TF	249.1230
	b3++ (P4)	DLSNPSRYLCK/TFC	823.3745
	y2+ (P4)	GE	205.0817
	y4+ (P4)	NGGE	376.1454
	y7++ (P4)	DLSNPSRYLCK/FCVNGGE	1009.4565
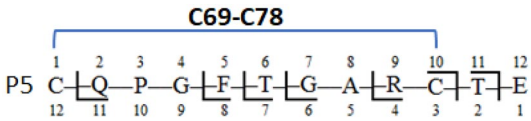	c10+ (P5)	CQPGFTGARC	1036.4407
	z4+ (P5)	RCTE	490.1827
	z·6+ (P5)	GARCTE	619.2482
	z·7+ (P5)	TGARCTE	720.2955
	z·8+ (P5)	FTGARCTE	867.3642

*In ETD fragmentation, the radical-induced backbone cleavage produces c and z·ions, as well as b· and y ions. The loss of CO from a b ion produces an a·ion (a + 1). An H·transfer from y to b·produces y·(y–1). The loss of an H·from z·forms z (z·–1). The column on the right presents the experimental m/z. This list comprises all MS/MS fragments annotated in Fig. 3

all three disulfide bonds peptides were detected in large peptide abundance (MS1 area > 10^6). The assignment of the MS/MS spectra of the disulfide bond-containing peptides are shown in Fig. 3. A list of the fragment ions annotated in the MS/MS spectra of the peptides identified with one disulfide bond identified in Fig. 3 is described in detail in Table 1. Identification of each ion fragment is given in the table column named fragmentation, with the corresponding amino acid sequence mass/charge described on the right for each annotated fragment.

The hNRG1α EGF domain is biologically active and promotes cell proliferation and migration

To determine if the recombinant hNRG1α EGF domain possesses intrinsic biological activity, its effect on cell proliferation was initially examined by a flow cytometry assay. The same number of HeLa cells was inoculated in both hNRG1α EGF domain-treated and untreated wells, with the treated wells receiving 50 ng/mL of hNRG1α EGF domain. The effect on proliferation was evaluated after 48 h, showing over a three-fold increase in cell number in the cultures treated with the recombinant hNRG1α EGF domain (Fig.4 A). Then, we performed a MTT based assay, which measures the reduction of a tetrazolium component (MTT) into an insoluble formazan product by the mitochondria, indirectly reflecting the number of viable cells. HeLa cells were cultivated with increasing concentrations of recombinant hNRG1α EGF domain to determine its capability to induce cell proliferation. The growth rate of cultures treated with concentrations as low as 0.05–0.5 ng/mL is significantly higher than the growth rate of control cells (Fig. 4B).

The activity of the recombinant hNRG1α EGF domain was also evaluated regarding cell migration by determining the gap closure rate of a scratch generated in NDFH cell monolayers (Fig. 4 C-D). The number of cells in the scratch zone was determined in the moment of gap generation and after 48 h. The gap closure rate was significantly higher in the NDFH cultures treated with the recombinant hNRG1α EGF domain as compared to the control cultures (Fig. 4D). These experiments show that the recombinant hNRG1α can induce both cell proliferation and migration.

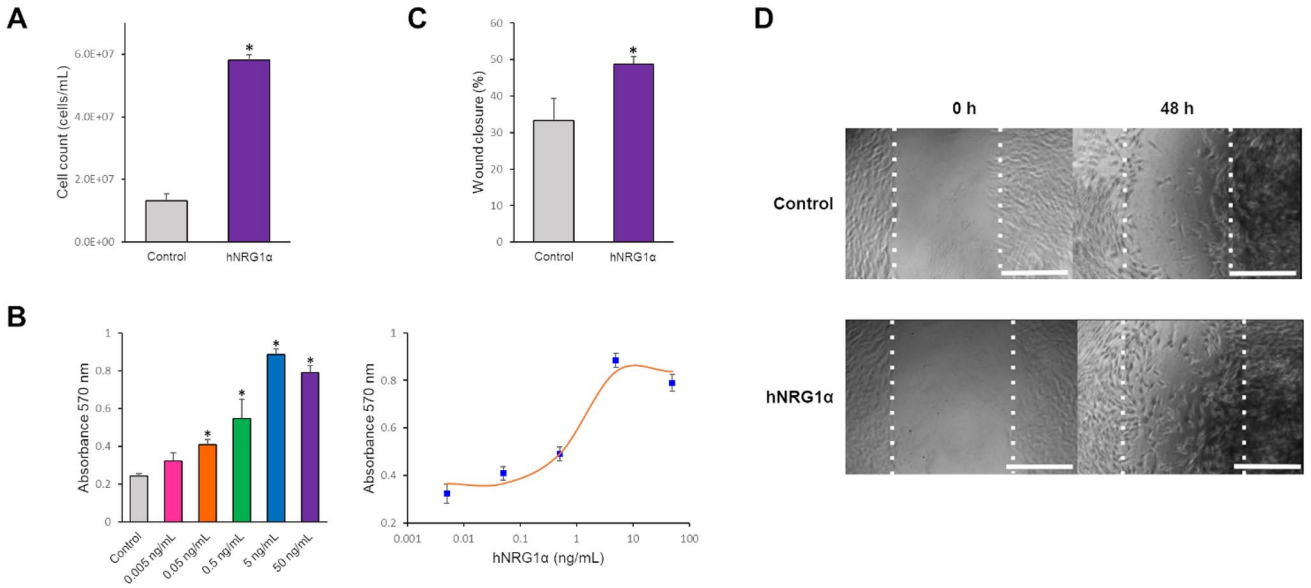

Fig. 4 Analysis of the biological activity of the recombinant hNRG1α EGF domain on cell proliferation and migration. (**A**) Comparison of the proliferation rate of HeLa cells treated with saturating concentration (50 ng/mL) of recombinant hNRG1α EGF domain with HeLa cell control cultures. Asterisk indicates $p < 0.05$. (**B**) HeLa cell proliferation induced by the hNRG1α EGF domain as determined by the MTT assay. Triplicate cultures of HeLa cells were treated with the indicated amounts of the hNRG1α EGF domain, and absorbance at 570 nm was measured after 48 h. The right panel shows the data fitting using a nonlinear regression. Asterisk indicates $p < 0.05$. (**C**) Analysis of the EGF-domain of hNRG1α activity on cell migration based on a scratch closure assay. The area of the wound in the moment of scratch generation was compared with the area after 48 h of incubation with 50 ng/mL of hNRG1α EGF domain. Control samples correspond to the same experimental conditions in absence of hNRG1α EGF domain. The assays were performed in triplicate. (**D**) Representative microscopy images of the scratch closure assay. The images at 100 X magnification were acquired at time 0 from native cells and after 48 h from fixed cells stained with violet crystal. The vertical doted lines indicate the border of the gap at time 0. Scale bar: 100 µm

Discussion

Neuregulins comprise a family of growth factors which, together with their ErbB receptors are involved in numerous neurodevelopmental processes and nervous system activities (for reviews see [2–4, 28]). NRG1 is expressed in neuronal and non-neuronal cell types and is responsible for cell maintenance, proliferation and migration [2, 3]. NRG2 promotes neuronal survival [29] and NRG3 has been associated with schizophrenia [30]. Six neuregulin genes have been identified in human cells, each giving rise to multiple isoforms originating from alternative splicing. Most neuregulins are synthesized as transmembrane proteins, which subsequently undergo proteolytic processing releasing the EGF signaling domain with different N-terminal domains [2, 3, 6]. The EGF domain of neuregulins was shown to be sufficient to activate ErbB receptors in a specific manner [8] and induce cellular responses in vitro [7].

The EGF domain comprises six cysteine residues separated by a constant number of residues (CX7CX4-5CX10-13CXCX8C) with the six conserved cysteines forming three disulfide bonds in the C1-C3, C2-C4, and C5-C6 combination [15]. Previous studies have described the expression in *E. coli* of the EGF domains fused only to affinity purification tags for some members of the EGF family [12–14]. However, the downside of such an approach was the limited solubility of the final product, and therefore, the necessity to purify inclusion bodies and to perform refolding in vitro to obtain a biologically active protein. A major reason to avoid larger N- and C-terminal tags is because they can cause a steric hindrance during the ligand-receptor interaction. To overcome both solubility and large-size tag problems, it is possible to express the protein of interest in fusion with chaperone proteins and include cleavage sites for specific proteases in the linker connecting the two proteins for separation of the protein of interest after purification. In this work, we have used the pET32a expression vector with the EGF domain of hNRG1α fused to the C-terminus of thioredoxin-A (TrxA). Upstream of the hNRG1α EGF domain, the genetic construction includes cleavage sites for enterokinase and thrombin proteases and a hexa-histidine tag. As expected, TrxA has a strong contribution for high levels of soluble expression (Fig. 1), which indicates also proper folding of the recombinant fusion protein. To avoid subsequent interference of the TrxA moiety, the fusion protein was separated by digestion with thrombin and TrxA, which keeps the hexa-histidine tag, was removed by affinity using an immobilized nickel column. This strategy turned out to be very efficient for production of soluble hNRG1α EGF domain.

Conformational stability and correct pairing of cysteines forming disulfide bonds were evaluated using several different approaches. Narhi et al. [31] demonstrated that when EGF is reduced, it goes through a considerable conformational change. Thus, when submitted to a reduced milieu these conformational changes can possibly lead to an easier access to the proteolytic sites by trypsin, which was confirmed by the comparison of the degradation pattern presented by the hNRG1α EGF domain in presence and absence of a reducing agent. A higher resistance to proteolytic digestion in absence of reducing agent is an indication of a compact conformation. Dynamic light scattering analyses in presence and absence of reducing agent revealed only small changes in the hydrodynamic radius, which increased from 2.4 to 2.7 nm. The hydrodynamic behavior of the hNRG1α EGF domain did not change even after long incubation times in presence of reducing agent nor after submission to a thermal ramp from 20 to 95 °C. The fact that only small changes in the hydrodynamic radius are detected is intriguing because more aggregation would be expected under reducing conditions. However, it seems that not all EGF domains aggregate after disulfide bond reduction. In an analysis of the hydrodynamic radius of seven different EGF domains reported previously [20], a similar behavior was observed for the recombinant EGF domain of hAREG and hHBEGF and hTGFa show only partial aggregation even after long incubation times (24 and 44 h) under reduction conditions, indicating that different EGF domains may present different solubility behavior under reducing conditions [20].

Conformation changes on the hNRG1α EGF domain were detected only by circular dichroism at high temperature (Fig. 2). These results indicate a highly stable conformation and solubility for the recombinant hNRG1α EGF domain.

Mapping disulfide bonds is a challenging task due to the reactive nature of thiol groups. In the case of the EGF domain, the compact nature of its folded structure adds up to the difficulties to obtain high quality peptide preparations for mass spectrometry. Nevertheless, peptides containing correct cysteine pairing were detected in high abundance for all three disulfide bonds, further supporting the evidence that the recombinant hNRG1α EGF domain produced in this work is properly folded.

After obtaining evidence that the hNRG1α EGF domain presents proper folding, we assessed its biological activity by determining its ability to induce cellular proliferation and migration cell culture assays. Both the proliferation rate determined by direct cell count and cell viability determined by MTT assays revealed a steady increase in cell growth. The data obtained in this work agree with previous observations where members of the EGF family recombinantly produced were shown to positively induce proliferation processes in several different cell lineages in the same concentration range [32–34], as low as 0,1 nM in the case of hEGF [35]. In the MTT assay there was a

slightly less proliferation at 50 ng/mL when compared with 5 ng/mL. That phenomenon was already demonstrated by other works [36], when higher concentrations lead to lower absorbance in the MTT assay. In a similar fashion, scratch gap closure assays were performed to measure the migratory capacities of the cells treated with saturating amounts of the hNRG1α EGF domain. Gap closure assays are useful to determine cell migration although in the case of fibroblast lineages such as NDFH (normal human dermal fibroblasts), proliferation and migration are usually linked. These assays showed that the hNRG1α EGF domain significantly induces faster gap closure than untreated control cells. Together, these assays show that the recombinant hNRG1α EGF domain presents the expected biological activity on cell proliferation and migration.

In addition to its role in the development and activity of the nervous system, NRG1 has been shown to play a central function in other processes including in nervous system injury recovery and repair [37–39], cardiac remodeling [40] and on the proliferation, migration, and angiogenesis of human periodontal ligament stem cells [10, 41]. The pathways underlining the processes modulated by NRG1/ErbB signaling are currently being investigated using reconstituted in vitro systems. In this context, the recombinant hNRG1α EGF domain can be a handy tool for studies designed to fill the molecular gaps between the step of ligand-receptor interaction up to the final biological outcome.

In summary, the strategy adopted in this work, combining high expression mediated by an expression chaperone with proteolytic separation of the chaperone consists in an efficient procedure to obtain the recombinant hNRG1α EGF domain, displaying correct disulfide bonds and functional properties similar to those described for its biologically functional counterparts. This recombinant growth factor can be readily produced to be used in functional experiments intended to expand the knowledge of the NRG1-ErbB signaling pathway.

Supplementary Information The online version contains supplementary material available at https://doi.org/10.1007/s11033-022-07956-3.

Acknowledgements The authors acknowledge the FIOCRUZ program of technical platforms for the support provided by the facilities for Protein Purification and Characterization (RPT15A), Mass Spectrometry (RPT02H) and Cytometry (RPT08L). The authors acknowledge Natália Salazar de Castro for providing plasmids pET22b-EGF and pET28a-TGFα and Eloise Pavão Guerra-Slompo for subcloning hNRG1α from pET32a- hNRG1α into plasmid pET28a.

Author contributions All authors contributed to the study conception and design. AL, ASF and NFB performed protein expression and purification experiments. ASF and BGG performed the biophysical characterizations and data analysis. MB performed mass spectrometry data acquisition and analysis. ASF and PMH performed the activity assays. ASF, BGG, MB, PMH and NITZ analyzed the results. AL and NITZ prepared the first draft of the manuscript. All authors reviewed the manuscript and approved its final version.

Funding This work was partially funded by the ICC-CNPq-PROEP Grant Number 442320/2019-1. ASF and AL were supported by CNPq (140923/2018-7) and CAPES graduate fellowships, respectively. NITZ and BGG are supported by Conselho Nacional de Desenvolvimento Científico e Tecnológico (CNPq) research career fellowships (304167/2019-3 and 304788/2018-0).

Data availability The datasets and reagents generated during this study are available from the corresponding author on reasonable request.

Declarations

Conflict of interest The authors have no relevant financial or non-financial interests to disclose.

Ethical approval Not applicable.

Consent to participate Not applicable

Consent to publish Not applicable.

References

1. Meyer D, Yamaal T, Garratt A et al (1997) Isoform-specific expression and function of neuregulin. Development 124:3575–3586. https://doi.org/10.1242/dev.124.18.3575
2. Mei L, Xiong WC (2008) Neuregulin 1 in neural development, synaptic plasticity and schizophrenia. Nat Rev Neurosci 9:437–452. https://doi.org/10.1038/nrn2392
3. Mei L, Nave KA (2014) Neuregulin-ERBB signaling in the nervous system and neuropsychiatric diseases. Neuron 83:27–49. https://doi.org/10.1016/j.neuron.2014.06.007
4. Cespedes JC, Liu M, Harbuzariu A, Annette N et al (2018) Neuregulin in health and disease. Int J Brain Disord Treat. https://doi.org/10.23937/2469-5866/1410024
5. Falls DL (2003) Neuregulins: Functions, forms, and signaling strategies. Exp Cell Res 284:14–30. https://doi.org/10.1016/S0014-4827(02)00102-7
6. Kao WT, Wang Y, Kleinman JE et al (2010) Common genetic variation in neuregulin 3 (NRG3) influences risk for schizophrenia and impacts NRG3 expression in human brain. Proc Natl Acad Sci U S A 107:15619–15624. https://doi.org/10.1073/pnas.1005410107
7. Pinkas-Kramarski R, Shelly M, Glathe S et al (1996) Neu differentiation factor/neuregulin isoforms activate distinct receptor combinations. J Biol Chem 271:19029–19032. https://doi.org/10.1074/jbc.271.32.19029
8. Carraway KL, Weber JL, Unger MJ, Ledesma J, Yu N, Gassmann M CL (1997) Neuregulin-2, a new ligand of ErbB3/ErbB4-receptor tyrosine kinases. Nature 387:512–516. https://doi.org/10.1007/3-540-29623-9_3120
9. Zhang D, Sliwkowski MX, Mark M et al (1997) Neuregulin-3 (NRG3): a novel neural tissue-enriched protein that binds and activates ErbB4. Proc Natl Acad Sci U S A 94:9562–9567. https://doi.org/10.1073/pnas.94.18.9562
10. Jones JT, Akita RW, Sliwkowski MX (1999) Binding specificities and affinities of egf domains for ErbB receptors. FEBS Lett 447:227–231. https://doi.org/10.1016/S0014-5793(99)00283-5

11. Rosano GL, Ceccarelli EA (2014) Recombinant protein expression in Escherichia coli: advances and challenges. Front Microbiol 5:1–17. https://doi.org/10.3389/fmicb.2014.00172
12. Mautino B, Costa LD, Gambarotta G et al (2004) Bioactive recombinant neuregulin-1, -2, and – 3 expressed in Escherichia coli. Protein Expr Purif 35:25–31. https://doi.org/10.1016/j.pep.2003.12.012
13. Abdull Razis AF, Ismail EN, Hambali Z et al (2008) Expression of recombinant human epidermal growth factor in Escherichia coli and characterization of its biological activity. Appl Biochem Biotechnol 144:249–261. https://doi.org/10.1007/s12010-007-8019-9
14. Song IJ, Ikram M, Subhan F et al (2015) Molecular characterization and expression analysis of mouse epidermal growth factor-like domain 8. Int J Mol Med 36:541–550. https://doi.org/10.3892/ijmm.2015.2252
15. Schneider MR, Wolf E (2009) The epidermal growth factor receptor ligands at a glance. J Cell Physiol 218:460–466. https://doi.org/10.1002/jcp.21635
16. Lu W, Cao P, Lei H, Zhang S (2010) High-level expression and purification of heparin-binding epidermal growth factor (HB-EGF) with SUMO fusion. Mol Biotechnol 44:198–203. https://doi.org/10.1007/s12033-009-9226-0
17. Qiang W, Gao T, Lan X et al (2020) Molecular pharming of the recombinant protein hegf-hegf concatenated with oleosin using transgenic arabidopsis. Genes (Basel) 11:1–13. https://doi.org/10.3390/genes11090959
18. Zheng X, Wu X, Fu X et al (2016) Expression and purification of human epidermal growth factor (hEGF) fused with GB1. Biotechnol Biotechnol Equip 30:813–818. https://doi.org/10.1080/13102818.2016.1166984
19. Kado Y, Mizohata E, Nagatoishi S et al (2016) Epiregulin recognition mechanisms by anti-epiregulin antibody 9E5: Structural, functional, and molecular dynamics simulation analyses. J Biol Chem 291:2319–2330. https://doi.org/10.1074/jbc.M115.656009
20. Ferreira AS, Lopacinski A, Batista M et al (2022) A toolkit for recombinant production of seven human EGF family growth factors in active conformation. Sci Rep 12:1–14. https://doi.org/10.1038/s41598-022-09060-9
21. Oliveira C, Domingues L (2018) Guidelines to reach high-quality purified recombinant proteins. Appl Microbiol Biotechnol 102:81–92. https://doi.org/10.1007/s00253-017-8623-8
22. Nagata K, Kohda D, Hatanaka H et al (1994) Solution structure of the epidermal growth factor-like domain of heregulin-α a ligand for p180(erbB-4). EMBO J 13:3517–3523. https://doi.org/10.1002/j.1460-2075.1994.tb06658.x
23. Hanahan D (1983) Studies on transformation of Escherichia coli with plasmids. J Mol Biol 166:557–580. https://doi.org/10.1016/S0022-2836(83)80284-8
24. Lobstein J, Emrich CA, Jeans C et al (2012) SHuffle, a novel Escherichia coli protein expression strain capable of correctly folding disulfide bonded proteins in its cytoplasm. Microb Cell Fact 11:1–16. https://doi.org/10.1186/s12934-016-0512-9
25. Feoktistova M, Geserick P, Leverkus M (2016) Crystal violet assay for determining viability of cultured cells. Cold Spring Harb Protoc 2016:343–346. https://doi.org/10.1101/pdb.prot087379
26. Abràmoff MD, Magalhães PJ, Ram SJ (2005) Image processing with imageJ Part II. Biophotonics Int 11:36–43
27. LaVallie ER, DiBlasio EA, Kovacic S et al (1993) A thioredoxin gene fusion expression system that circumvents inclusion body formation in the E. coli cytoplasm. Bio/Technology 11:187–193. https://doi.org/10.1038/nbt0293-187
28. Buonanno A (2010) The neuregulin signaling pathway and schizophrenia: from genes to synapses and neural circuits. Brain Res Bull 83:122–131. https://doi.org/10.1016/J.BRAINRESBULL.2010.07.012
29. Kim JA, Jayabalan AK, Kothandan VK et al (2016) Identification of Neuregulin-2 as a novel stress granule component. BMB Rep 49:449–454. https://doi.org/10.5483/BMBRep.2016.49.8.090
30. Wang YC, Chen JY, Chen ML et al (2008) Neuregulin 3 genetic variations and susceptibility to Schizophrenia in a Chinese population. Biol Psychiatry 64:1093–1096. https://doi.org/10.1016/j.biopsych.2008.07.012
31. Narhi LO, Arakawa T, McGinley MD et al (1992) Circular dichroism of reduced and oxidized recombinant human epidermal growth factor. Int J Pept Protein Res 39:182–187. https://doi.org/10.1111/j.1399-3011.1992.tb00786.x
32. Mvula B, Moore TJ, Abrahamse H (2010) Effect of low-level laser irradiation and epidermal growth factor on adult human adipose-derived stem cells. Lasers Med Sci 25:33–39. https://doi.org/10.1007/s10103-008-0636-1
33. Yoneda N, Sato Y, Kitao A et al (2011) Epidermal growth factor induces cytokeratin 19 expression accompanied by increased growth abilities in human hepatocellular carcinoma. Lab Investig 91:262–272. https://doi.org/10.1038/labinvest.2010.161
34. Inatomi O, Andoh A, Yagi Y et al (2006) Regulation of amphiregulin and epiregulin expression in human colonic subepithelial myofibroblasts. Int J Mol Med 18:497–503. https://doi.org/10.3892/ijmm.18.3.497
35. Strachan L, Murison JG, Prestidge RL et al (2001) Cloning and biological activity of Epigen, a novel member of the epidermal growth factor superfamily. J Biol Chem 276:18265–18271. https://doi.org/10.1074/jbc.M006935200
36. O'Rourke DM, Qian X, Zhang HT et al (1997) Trans receptor inhibition of human glioblastoma cells by erbB family ectodomains. Proc Natl Acad Sci U S A 94:3250–3255. https://doi.org/10.1073/pnas.94.7.3250
37. Kataria H, Karimi-Abdolrezaee S (2017) Neuregulin-1: a novel regulator of glial response in spinal cord injury. Neural Regen Res 12:1616–1617. https://doi.org/10.4103/1673-5374.217331
38. Alizadeh A, Dyck SM, Kataria H et al (2017) Neuregulin-1 positively modulates glial response and improves neurological recovery following traumatic spinal cord injury. Glia 65:1152–1175. https://doi.org/10.1002/GLIA.23150
39. Kataria H, Alizadeh A, Karimi-Abdolrezaee S (2019) Neuregulin-1/ErbB network: an emerging modulator of nervous system injury and repair. Prog Neurobiol. https://doi.org/10.1016/J.PNEUROBIO.2019.101643
40. Dugaucquier L, Feyen E, Mateiu L et al (2020) The role of endothelial autocrine NRG1/ERBB4 signaling in cardiac remodeling. Am J Physiol - Hear Circ Physiol 319:H443–H455. https://doi.org/10.1152/ajpheart.00176.2020
41. Li L, Shang L, Kang W et al (2022) Neuregulin-1 promotes the proliferation, migration, and angiogenesis of human periodontal ligament stem cells in vitro. Cell Biol Int. https://doi.org/10.1002/CBIN.11770